

⁸This is in disagreement with the spacings found in reference 2.

⁹P. E. Golden and D. Rapp, Lockheed Missiles and

Space Company Technical Report No. 6-74-64-12 (unpublished); D. D. Briglia and D. Rapp, Phys. Rev. Letters 14, 245 (1965).

LASER DOUBLE-QUANTUM PHOTODETACHMENT OF I^-

J. L. Hall, E. J. Robinson, and L. M. Branscomb

Joint Institute for Laboratory Astrophysics,* Boulder, Colorado

(Received 7 May 1965)

Since the advent of lasers, many types of multiple-photon absorption processes have been investigated,¹⁻⁴ principally between bound states in solids. We report here the results of an experimental study of two-quantum induced photodetachment of electrons from a beam of negative ions of atomic iodine (I^-) in high vacuum. Because of the simplicity of the energy level spectrum of I^- (only one bound state, at -3.076 eV), it might be expected that rather detailed comparison of experimental results with theory should be feasible.

For completeness, we summarize here briefly the theoretical situation. The transition probability per second for a two-photon absorption process is given by

$$W_2 = \frac{2\pi}{\hbar} \left| \sum_n \frac{\langle i|H|n\rangle \langle n|H|f\rangle}{(E_i + 2h\nu) - (E_n + h\nu)} \right|^2 \rho(E), \quad (1)$$

where H is the interaction Hamiltonian, $\rho(E)$ is the density of final states, and E_i and E_n are the energies of $|i\rangle$ and $|n\rangle$. Geltman⁵ has evaluated Eq. (1) for transitions from the single bound state of (atomic) halogen negative ions to the continuum, using the plane-wave approximation for the free-electron states. A particularly simple result is obtained in this approximation, since the only intermediate state $|n\rangle$ which contributes to the sum in Eq. (1) is the state $|n\rangle = |f\rangle$. This makes W_2 proportional to the known single-quantum photodetachment cross section σ at twice the laser frequency. Using the measured⁶ value of σ , Geltman's result may be written

$$W_2 = \delta F^2 \text{ with } \delta = 5 \times 10^{-51} \text{ cm}^4 \text{ sec},$$

where the photon flux F is in photons $\text{cm}^{-2} \text{sec}^{-1}$. For our typical $\frac{1}{3}$ - μA beam of 500-eV ions focused through an area 0.1 cm^2 and crossed by a 1-J, 20-MW Q-switched ruby laser focused through an area 10^{-2} cm^2 , this value of δ leads

to an expectation of about 30 double-quantum photodetached electrons per laser pulse.

We describe here a measurement of the value of δ at $h\nu = 1.785$ eV, using the apparatus schematically depicted in Fig. 1.⁷ Iodine negative ions are generated in a hot cathode arc discharge operated in ammonia and I_2 vapor at 30μ pressure. Negative ions are extracted, accelerated, mass-analyzed, slowed, and then focused by an "einzel" lens into an area of about 9 mm^2 where they are crossed with the laser beam. The detached electrons are focused onto the first dynode of an electron multiplier. Some difficulty was experienced with spurious electrons removed by the laser, perhaps thermally, from the silvered mirror which redirects the laser beam to the laser monitor external to the vacuum system. Biasing the interaction region a few volts negative effectively reduced collection of these spurious charges. The residual signal may just be seen in Fig. 2(b), and was never more than a few electrons. To

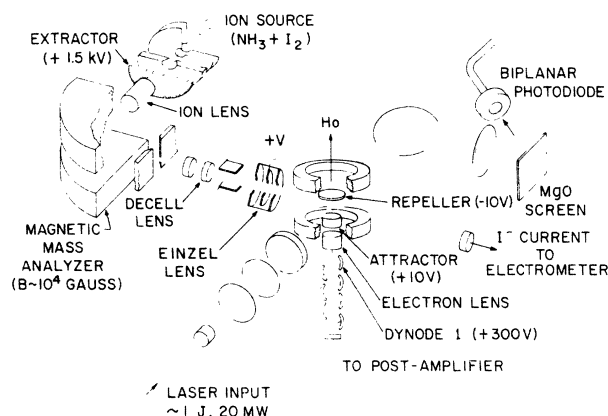


Fig. 1. Schematic diagram of the apparatus. For clarity the movable phosphor is not illustrated. The $\frac{1}{2}$ -in. diameter by 4-in. long optically excellent ruby was run close to threshold, being Q switched by a rotating plane mirror.

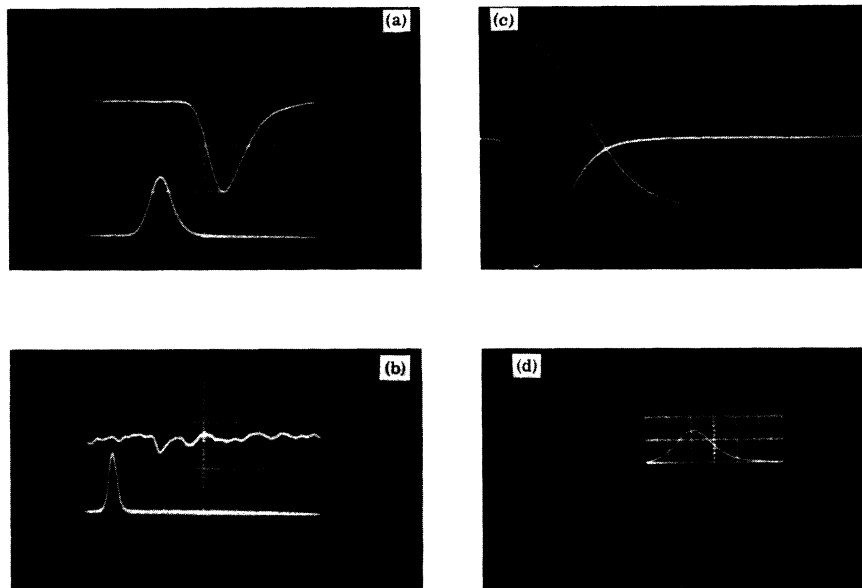


FIG. 2. Diagnostic and useful data. (a) Two-quantum electron signal, ion beam on, electron signal (upper trace) 30 electrons/division. Lower trace is laser output. Time base 49 nsec/division. Time delay is due to electron multiplier and postamplifier. (b) Background signal, ion beam off. Electron signal (upper trace) at 3 electrons/division. Time base 100 nsec/division. (c) Two-quantum data. Fast signal (lower trace) at 100 nsec/cm. Integral signal (upper trace) 30 electrons/division, 2 μ sec/division. Ion beam current 0.3 μ A. (d) Biplanar photocell output. 5.5 MW/cm. 20 nsec/cm.

eliminate errors due to transit-time spreading in the electron multiplier, the useful data were taken by integrating the output of the multiplier's postamplifier. Both the fast output and the integral were displayed on a dual-beam oscilloscope.

The possibility existed that the observed effect in iodine was single-quantum photodetachment due to uv second-harmonic photons generated in the optical components. Since no photodetachment signals were observed when a uv-passing, red-absorbing filter was inserted in the beam after the lenses, we conclude that a negligible second harmonic was generated by the lenses. Because the fractional second-harmonic generation should depend inversely on the laser-beam area, we expected no appreciable contribution from the vacuum window where the beam cross section is enlarged by a factor of 4. Furthermore, a duplicate window placed in the unmagnified beam still gave zero signal through the uv-pass filter. Thus we conclude that any second-harmonic light which might have been seen by the ions has negligible effect.

The laser power and its time dependence were measured with a very high-speed biplanar pho-

todiodide driving a traveling-wave oscilloscope. The absolute calibration of the photodiode was accomplished to about 5% by comparison with a liquid-cell calorimeter. This calorimeter contained a heater coil to allow experimental verification of the calculated specific heat. The geometry and spatial overlap of the ion and laser beams were studied with a movable phosphor screen which could be swung into position at 45° to both beams. By arranging the optical lenses to image an external iris into the interaction region, a very well-defined laser spot could be produced. Laser light and white light autocollimated through the ruby were shown to be precisely coincident, so that photographs of the actual spatial alignment could be made without operating the laser.

Calibration of the electron multiplier and collection optics was done in two steps. First we measured the pulse-height distribution and integral signals corresponding to a single electron incident on the first dynode. These electrons were collisionally detached from the ion beam by the $<10^{-7}$ -Torr background gas. Secondly, the electron-collection efficiency f was measured by saturating a weak beam of H^- ions with the Q -switched laser, using essentially

the same geometry as in the iodine experiments. The H^- single-quantum cross section and the laser flux are great enough that the process is strongly saturated; the probability that an H^- ion will lose its electron is essentially unity. This calibration is relatively insensitive to the precise values of cross section and laser flux, depending mainly on ion transit time through the light and the (measured) time dependence of the laser. As a check on systematic errors, the unsaturated photodetachment for H^- was measured with the attenuated output of the laser operating in the non- Q -switch mode. The cross section value thus obtained is equal within 5% (with a scatter of 10%) to the known H^- cross section.⁸

The data consist of photographs of the dual-beam and traveling-wave oscilloscope traces, such as Figs. 2(c) and 2(d). The number of electrons detached is proportional to the product of the voltage of the time-integral multiplier signal and the collection efficiency. The time integral of the square of the flux was obtained by numerical integration from the enlarged trace of the traveling-wave oscilloscope, knowing the laser spot size.

Figure 3 is a logarithmic plot of the number of detached electrons per illuminated ion versus the time integral of the square of the laser flux. The uncorrected value δ_0 of δ derived from these data is $(350 \pm 140) \times 10^{-51} \text{ cm}^4 \text{ sec}$. The assigned probable error is substantially greater than the probable error for a single measurement and represents our best judgment of possible uncorrected systematic errors. The two most serious problems appear to be the following: In Fig. 3, a slope of 1 is expected, but the measured slope is 1.12. This slight discrepancy, as the area of the laser beam was varied by a factor of 16, is related to the fact that the ion beam is not uniform, being somewhat less intense near its boundaries. Corrections deduced from the photography of images of the ion beam of the phosphor screen are of limited accuracy. The other possible source of error is the measured spatial decrease of the electron collection efficiency (which at the optimum is only 1/7).

To put this measurement on an absolute basis, some corrections for laser coherence effects must be made. For an ideal laser, producing a sinusoidal electric field, the value of the flux-squared integral as obtained above

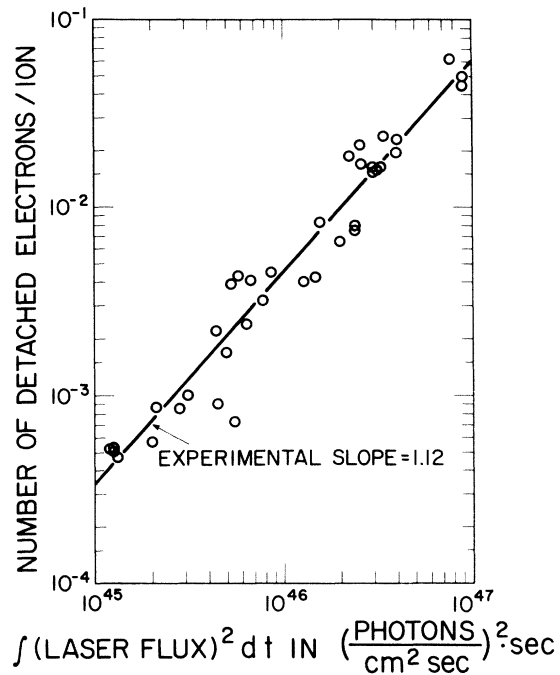


Fig. 3. Integrated photodetachment probability versus $\int F^2 dt$. No experimental points have been omitted. The laser output varied about a factor of 10 due to alignment changes and incomplete cooling. The effective area of the laser spot was varied by changing the focusing conditions. This plot does not contain the corrections for laser coherence.

must be corrected upward by the factor $\frac{3}{2}$, this being the ratio of $\langle \cos^4 ut \rangle$ to $\langle \cos^2 ut \rangle^2$. An additional upward correction of $h \equiv (2n-1)/n$ arises if the laser is operating multimode.⁹ Here n is the effective number of modes simultaneously influencing the iodine ion. Because the ions travel through an image of the near field of the filament-like ruby, they experience the spatial multimode character of the laser mainly sequentially, not simultaneously. There is probably some overlap of these bright zones, and there were often two discrete laser frequencies produced. In view of these uncontrollable effects, we will assume an average value of $h = (1.3 \pm 0.3)$, which includes both $n=1$ and $n=2$. The scatter evident in Fig. 3 is much worse than in the single-photon hydrogen experiment, and is presumably due to the nonreproducible laser coherence properties. The final corrected value of δ is $\delta_C = \delta_0 \times [\frac{3}{2} \times (1.3 \pm 0.3)]^{-1}$ or $\delta_C = 180 \times 10^{-51} \text{ cm}^4 \text{ sec}$. The estimated uncertainty is a factor of 1.5.

Geltman's theoretical value of $5 \times 10^{-51} \text{ cm}^4$ lies far outside the range of the estimated experimental error, and it thus appears that the approximation of plane waves for continuum states is insufficient.

We are deeply indebted to D. A. Jennings of the National Bureau of Standards for the generous loan of some essential parts of the apparatus, as well as several helpful discussions. It is a pleasure to acknowledge the excellent craftsmanship of R. T. Weppner in the construction of the movable phosphor screen and other components.

†This research has been supported by the Advanced Research Projects Agency through the Office of Naval Research and the U. S. Army Research Office-Durham, as well as by the National Bureau of Standards.

*Of the National Bureau of Standards and the University of Colorado.

¹W. Kaiser and C. G. B. Garrett, Phys. Rev. Letters 7, 229 (1961).

²W. L. Peticolas, J. P. Goldsborough, and K. E. Rieckhoff, Phys. Rev. Letters 10, 43 (1963).

³J. L. Hall, D. A. Jennings, and R. M. McClintock, Phys. Rev. Letters 11, 364 (1963).

⁴H. Sonnenberg, H. Heffner, and W. Spicer, Appl. Phys. Letters 5, 95 (1964).

⁵S. Geltman, Phys. Letters 4, 168 (1963).

⁶B. Steiner, M. L. Seman, and L. M. Branscomb, J. Chem. Phys. 37, 1200 (1962).

⁷The basic ion-beam machine has been used previously for single-quantum photodetachment experiments by Branscomb and others. See, e.g., M. L. Seman and L. M. Branscomb, Phys. Rev. 125, 1602 (1962).

⁸S. Geltman, Astrophys. J. 136, 935 (1962).

⁹This factor was obtained also in the case of second-harmonic generation by A. Ashkin, G. D. Boyd, and J. M. Dziedzic, Phys. Rev. Letters 11, 14 (1963).

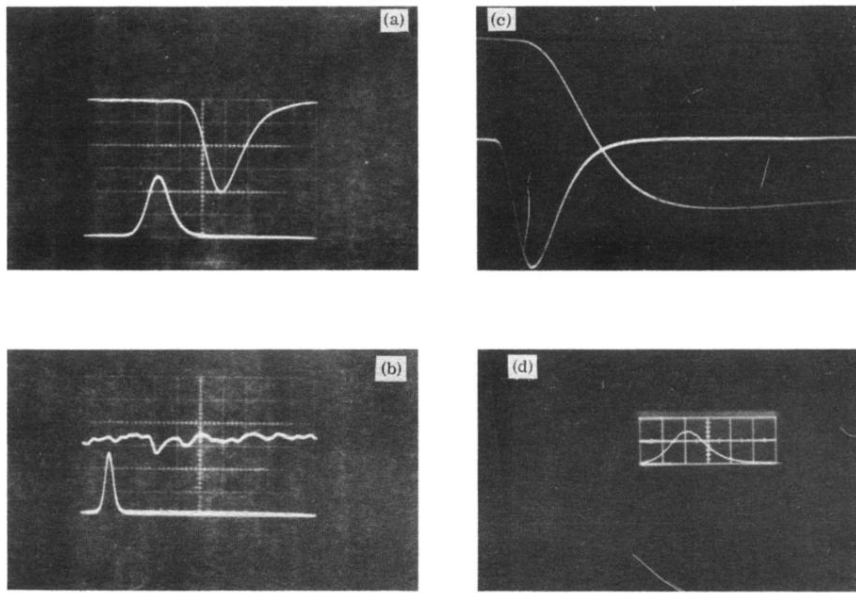


FIG. 2. Diagnostic and useful data. (a) Two-quantum electron signal, ion beam on, electron signal (upper trace) 30 electrons/division. Lower trace is laser output. Time base 49 nsec/division. Time delay is due to electron multiplier and postamplifier. (b) Background signal, ion beam off. Electron signal (upper trace) at 3 electrons/division. Time base 100 nsec/division. (c) Two-quantum data. Fast signal (lower trace) at 100 nsec/cm, Integral signal (upper trace) 30 electrons/division, 2 μ sec/division. Ion beam current 0.3 μ A. (d) Biplanar photocell output. 5.5 MW/cm. 20 nsec/cm.